J. Antibiot. 59(12): 777–784, 2006

ORIGINAL ARTICLE

THE JOURNAL OF ANTIBIOTICS

F-16438s, Novel Binding Inhibitors of CD44 and Hyaluronic Acid

II. Producing Organism, Fermentation, Isolation, Physico-chemical Properties and Structural Elucidation

Yuki Hirota-Takahata, Hosami Harada, Isshin Tanaka, Tomoko Nakata, Mutsuo Nakajima, Masaaki Takahashi

Received: August 11, 2006 / Accepted: November 14, 2006

Abstract In the course of our screening for binding inhibitors of CD44 and hyaluronic acid, five active compounds, F-16438 A, B, E, F and G were found and isolated from the cultured broth of a fungal strain, *Gloeoporus dichrous* SANK 30502. The structures of these compounds except for F-16438 G were elucidated by physico-chemical and spectral data to be new compounds related to caloporoside; F-16438 G was identified to be the 6'-malonylated derivative of caloporoside.

Keywords F-16438, hyaluronic acid, CD44, binding inhibitor, caloporoside

Introduction

Hyaluronic acid (HA) is a high-molecular-weight polysaccharide, composed of a multiple repeat of glucuronic acid and *N*-acetylglucosamine, principally produced by stromal cells and deposited in the extracellular matrix (ECM) of most tissues. HA is a major molecule in joint fluid [1] and plays a crucial role in joint motion and homeostasis [2]. In fact, the concentration and average molecular weight of HA in the joint fluids are reduced in osteoarthritis and rheumatoid arthritis [3, 4]. It has also been shown that HA participates in inflammation [5, 6], tumor progression and invasion [7, 8]. In highly invasive breast cancer cell lines, not only synthesis but also HA degradation is upregulated [9].

CD44 is the most common HA receptor and is expressed abundantly on many cell types [10～15]. CD44 has been shown to mediate cell-cell and cell-ECM interaction *via* its affinity to HA. It is also suggested that HA is incorporated into cells by CD44 for degradation [16～18]. Therefore, inhibition of the binding of HA to its receptor is expected to have high efficiency for the inhibition of HA function and/or turnover and might be of therapeutic value in the treatment of diseases such as cancer, osteoarthritis and rheumatoid arthritis.

In the course of our screening for binding inhibitors of CD44 and HA, potent activity was detected in the cultured broth of *Gloeoporus dichrous* SANK 30502; five active compounds, F-16438 A (**1**), B (**2**), E (**3**), F (**4**) and G (**5**) were isolated (Fig. 1).

In this paper, we report the producing organism, fermentation, isolation, physico-chemical properties and structural elucidations of F-16438s. Details of the biological activities of F-16438s were reported in a previous paper [19].

Results

Producing Organism

The producing strain SANK 30502 was isolated from the spore print of a fresh fruiting body collected in Kanagawa

M. Takahashi (Corresponding author)**, H. Harada, T. Nakata:** Lead Discovery Research Laboratories, Sankyo Co., Ltd., 1-2-58 Hiromachi, Shinagawa-ku, Tokyo 140-8710, Japan,
E-mail: mtakah@sankyo.co.jp

Y. Hirota-Takahata, I. Tanaka, M. Nakajima: Core Technology Research Laboratories, Sankyo Co., Ltd., 1-2-58 Hiromachi, Shinagawa-ku, Tokyo 140-8710, Japan

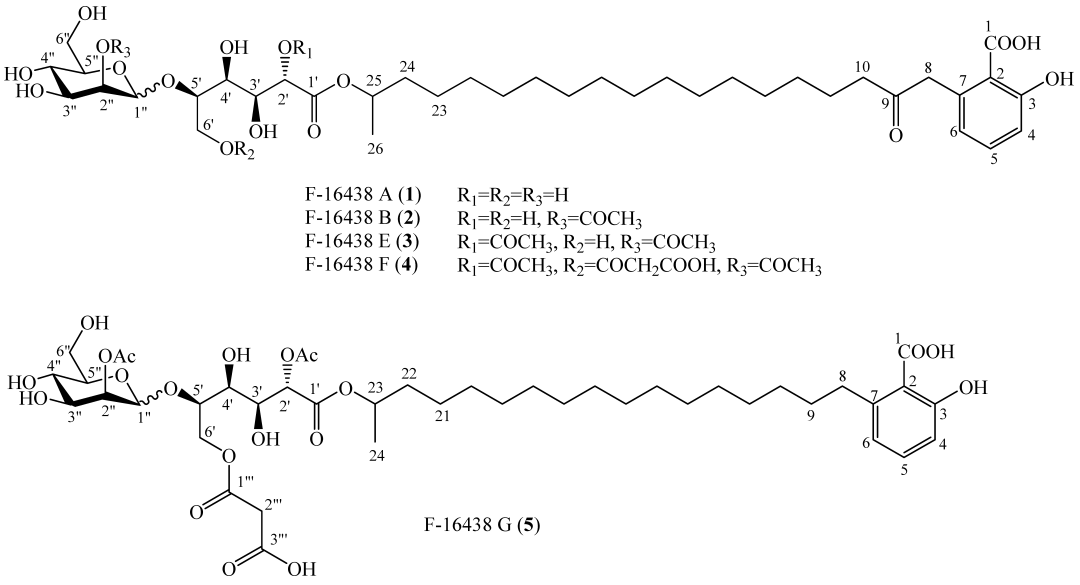

Fig. 1 Structures of F-16438s.

Prefecture, Japan. The characteristics of the fruiting body corresponded with the description of *Gloeoporus dichrous* (Fr.:Fr.) Bres. described by Núñez and Ryvarden [20]. The strain has been deposited at the National Institute of Advanced Industrial Science and Technology, Japan, as *Gloeoporus dichrous* SANK 30502 under the accession number FERM BP-8310.

Fermentation

The growth of *Gloeoporus dichrous* SANK 30502 on an agar slant was homogenized with sterile water (3 ml). Then the whole amount of the homogenate was transferred into a 100-ml Erlenmeyer flask containing 30 ml of a primary seed medium, which was composed of glucose 0.4%, malt extract 1.0%, yeast extract 0.4%, agar 0.3% and Disfoam CB-442 (Nippon Yushi Co.) 0.005%, pH 5.5 before sterilization. The flask was incubated at 23°C for 7 days on a rotary shaker at 210 rpm. The primary seed culture (3 ml) was transferred into a 500-ml Erlenmeyer flask containing 80 ml of a sterilized production medium which was composed of maltose 2.0%, glucose 1.0%, polypeptone 0.2%, yeast extract 0.08%, KH_2PO_4 0.05%, $MgSO_4 \cdot 7H_2O$ 0.1%, $FeCl_3 \cdot 6H_2O$ 0.001%, $ZnSO_4 \cdot 7H_2O$ 0.0002%, $CaCl_2$ 0.0055%, Disfoam CB-442 0.005%. The fermentation was carried out at 23°C for 14 days on a rotary shaker at 210 rpm.

Isolation

An equal amount of acetone was added to the cultured broth (160 ml). The extract was filtered with the assistance of Celite 545 and the filtrate was concentrated to remove the acetone. The pH of the concentrate was adjusted to 3.0 with 6 N HCl, and the active compounds were extracted with ethyl acetate (150 ml). The organic layer was washed with brine, dried over anhydr. Na_2SO_4, and concentrated to dryness to give an oily substance (209 mg). To prepare a column charge, the substance was dissolved in 3 ml of methanol and adsorbed to a 2 g portion of Cosmosil 140C18-OPN. After removal of the methanol, the charge was suspended in a small amount of MeCN - 0.3% triethylamine-phosphate (TEAP) buffer at pH 3.0 (3 : 7) and was embedded to the Cosmosil 140C18-OPN column (30 ml). The chromatography was performed by stepwise elution using MeCN - 0.3% TEAP buffer at pH 3.0 in the ratio 3 : 7, 2 : 3 and 1 : 1, 150 ml each.

1) Isolation of F-16438 A (**1**) and B (**2**)

The part of the ratio 1 : 1 eluate containing **1** and **2** on the Cosmosil column chromatography, was concentrated to remove the MeCN. These two compounds were extracted with ethyl acetate and the organic layer was washed with brine, dried over anhydr. Na_2SO_4, and concentrated to dryness to obtain crude material (43.4 mg). Finally, they were purified by preparative HPLC using an ODS column (Waters, SYMMETRY C18 19 i.d.×100 mm). The chromatography was performed with 55% MeCN in 0.02% aq. formic acid at a flow rate of 6 ml/minute. Each fraction containing **1** or **2** was collected and concentrated to dryness, yielding 6.1 mg of **1** and 13.5 mg of **2**, respectively.

Table 1 Physico-chemical properties of F-16438s

	F-16438 A (**1**)	F-16438 B (**2**)	F-16438 E (**3**)
Appearance	White powder	White powder	White powder
Molecular formula	$C_{38}H_{62}O_{16}$	$C_{40}H_{64}O_{17}$	$C_{42}H_{66}O_{18}$
HR-MS (*m/z*)			
Found:	797.3923 $(M+Na)^+$	839.4089 $(M+Na)^+$	881.4174 $(M+Na)^+$
Calcd.:	797.3936 (for $C_{38}H_{62}O_{16}Na$)	839.4041 (for $C_{40}H_{64}O_{17}Na$)	881.4147 (for $C_{42}H_{66}O_{18}Na$)
$[\alpha]_D^{22}$ (*c* 1.0, MeOH)	−18°	−29°	−29°
UV λ_{max}^{MeOH} nm (ε)	207 (29700), 243 (sh, 4600), 306 (3900)	208 (32000), 242 (sh, 4900), 306 (4300)	208 (29900), 242 (sh, 4700), 306 (3900)
IR ν_{max} (KBr) cm^{-1}	3377, 2923, 2852, 1726, 1663, 1465, 1379, 1216, 1074, 1029	3390, 2925, 2853, 1730, 1671, 1465, 1376, 1249, 1075, 1031	3418, 2927, 2855, 1738, 1672, 1465, 1375, 1231, 1075, 1032
HPLC (Rt. minute)	3.6[a)]	4.8[a)]	7.5[a)]

	F-16438 F (**4**)	F-16438 G (**5**)
Appearance	White powder	White powder
Molecular formula	$C_{45}H_{68}O_{21}$	$C_{43}H_{66}O_{20}$
HR-MS (*m/z*)		
Found:	967.4180 $(M+Na)^+$	925.4086 $(M+Na)^+$
Calcd.:	967.4151 (for $C_{45}H_{68}O_{21}Na$)	925.4045 (for $C_{43}H_{66}O_{20}Na$)
$[\alpha]_D^{22}$ (*c* 1.0, MeOH)	−23°	−26°
UV λ_{max}^{MeOH} nm (ε)	208 (29400), 243 (sh, 4700), 307 (4200)	208 (29000), 241 (sh, 4500), 305 (3200)
IR ν_{max} (KBr) cm^{-1}	3421, 2926, 2855, 1741, 1673, 1465, 1375, 1228, 1071	3408, 2924, 2853, 1739, 1661, 1453, 1377, 1242, 1068
HPLC (Rt. minute)	8.5[a)]	11.4[a)]

[a)] SYMMETRY C18 (Waters, 4.6 i.d.×150 mm), MeCN - 0.3% TEAP, pH 3 (3 : 2), 1 ml/minute.

2) Isolation of F-16438 E (**3**), F (**4**) and G (**5**)

The part of the ratio 1 : 1 eluate containing **3**, **4** and **5** on the Cosmosil column chromatography, was concentrated to remove the MeCN. These three compounds were extracted with ethyl acetate and the organic layer was washed with brine, dried over anhydr. Na_2SO_4, and concentrated to dryness (82.4 mg). Finally, they were purified by preparative HPLC using the same ODS column described above. The chromatography was performed with 60% MeCN in 0.02% aq. formic acid at a flow rate of 6 ml/minute. Each fraction containing **3** or **4** or **5** was collected and concentrated to dryness, yielding 21.9 mg of **3**, 29.1 mg of **4** and 2.8 mg of **5**, respectively.

Physico-chemical Properties of 1, 2, 3, 4 and 5

The physico-chemical properties of F-16438s are summarized in Table 1.

The molecular formulae of **1**, **2**, **3**, **4** and **5** were determined to be $C_{38}H_{62}O_{16}$ [*m/z*, found 797.3923 $(M+Na)^+$, calcd. 797.3936 for $C_{38}H_{62}O_{16}Na$], $C_{40}H_{64}O_{17}$ [*m/z*, found 839.4089 $(M+Na)^+$, calcd. 839.4041 for $C_{40}H_{64}O_{17}Na$], $C_{42}H_{66}O_{18}$ [*m/z*, found 881.4174 $(M+Na)^+$, calcd. 881.4147 for $C_{42}H_{66}O_{18}Na$], $C_{45}H_{68}O_{21}$ [*m/z*, found 967.4180 $(M+Na)^+$, calcd. 967.4151 for $C_{45}H_{68}O_{21}Na$], $C_{43}H_{66}O_{20}$ [*m/z*, found 925.4086 $(M+Na)^+$, calcd. 925.4045 for $C_{43}H_{66}O_{20}Na$], respectively, by positive ion ESITOF-MS.

Structural Elucidation of 3

The structural elucidation was mainly focused on **3**. The ^1H and ^{13}C NMR spectral data of **3** obtained in pyridine-d_5 are summarized in Table 3. In the ^1H NMR spectrum of **3**, signals from two acetyl groups (δ 1.82 and 2.19), the glycosyl group (δ 3.9∼6.2) and the phenyl group (δ 6.8∼7.5), were observed. In the region of the alkyl group, highly overlapped methylene or methyl proton signals were observed. In the ^{13}C NMR spectrum, 30 assignable carbon signals were observed and classified into 3× methyl, 7×

Table 2 ^{1}H and ^{13}C NMR signal assignments of F-16438 A (**1**) and F-16438 B (**2**) in pyridine-d_5

Position	F-16438 A (**1**)		F-16438 B (**2**)	
	δ_C	δ_H	δ_C	δ_H
1[a]				
2[a]				
3	164.0 (s)		163.8 (s)	
4	116.7 (d)	7.17 (1H, d, 8.3 Hz)	116.7 (d)	7.16 (1H, d, 8.3 Hz)
5	133.4 (d)	7.39 (1H, dd, 7.3, 8.3 Hz)	133.7 (d)	7.40 (1H, dd, 7.3, 8.3 Hz)
6	122.9 (d)	6.85 (1H, d, 7.3 Hz)	122.9 (d)	6.86 (1H, d, 7.3 Hz)
7	139.6 (s)		139.5 (s)	
8[a]		4.25 (2H, s)		4.21 (2H, s)
9[a]				
10	42.3 (t)	2.62 (2H, t, 7.3 Hz)	42.3 (t)	2.60 (2H, t, 7.5 Hz)
11	24.2 (t)	1.72 (2H, m)	24.2 (t)	1.72 (2H, m)
12~22	29.7~29.9 (t)	1.15~1.35 (22H[b])	29.7~30.0 (t)	1.14~1.26 (22H[b])
23	25.8 (t)	1.29 (2H, m)	25.8 (t)	1.31 (2H, m)
24	36.2 (t)	1.45 (1H, m), 1.63 (1H, m)	36.3 (t)	1.49 (1H, m), 1.69 (1H, m)
25	71.2 (d)	5.20 (1H, m)	71.2 (d)	5.23 (1H, m)
26	20.2 (q)	1.29 (3H, d, 6.0 Hz)	20.2 (q)	1.31 (3H, d, 6.5 Hz)
1′	174.8 (s)		174.6 (s)	
2′	72.3 (d)	5.24 (1H, d, 8.5 Hz)	73.4 (d)	5.16 (1H, s)
3′	73.6 (d)	5.16 (1H, d, 8.5 Hz)	72.2 (d)	5.16 (1H, s)
4′	70.4 (d)	4.88 (1H, d, 8.0 Hz)	70.4 (d)	4.77 (1H, s)
5′	81.6 (d)	4.77 (1H, br s)	80.4 (d)	4.77 (1H, s)
6′	63.8 (t)	4.29 (1H, dd, 7.0, 11.7 Hz) 4.59 (1H[b])	63.9 (t)	4.28 (1H, m), 4.62 (1H, m)
1″	102.4 (d)	5.37 (1H, s)	100.0 (d)	5.60 (1H, s)
2″	72.3 (d)	4.61 (1H, m)	73.4 (d)	6.14 (1H, d, 3.3 Hz)
3″	75.8 (d)	4.08 (1H, dd, 2.6, 9.4 Hz)	73.7 (d)	4.25 (1H, dd, 3.3, 9.5 Hz)
4″	69.6 (d)	4.40 (1H, dd, 9.4, 9.5 Hz)	69.6 (d)	4.39 (1H, dd, 9.0, 9.5 Hz)
5″	78.7 (d)	3.92 (1H, m)	78.6 (d)	3.97 (1H, m)
6″	63.4 (t)	4.21 (1H, dd, 7.7, 10.3 Hz) 4.59 (1H[b])	63.2 (t)	4.31 (1H, m), 4.64 (1H, m)
2″-OAc			171.1 (s)	
			21.3 (q)	2.10 (3H, s)

[a] ^{13}C signal was not clearly observed. [b] Overlapped.

methylene, 13× methine and seven quaternary carbons, as well as complexly overlapped methylene carbon signals in the alkyl region. In addition, one carbon signal assigned to a saturated carbonyl (C-9) as shown in Fig. 1 was not clearly observed in this solvent.

The partial structures, except for the alkyl chain and the bonds between C-1′ and C-2′, C-3′ and C-4′ of **3**, were elucidated by several NMR techniques such as DQFCOSY, HSQC and HMBC.

As the disappearance of the C-9 carbon signal interfered with the structural elucidation of the alkyl chain of **3**, its assignment was carried out by mass spectrometry and several NMR techniques performed on the decomposition product of **3** (**6**, Fig. 2), which was prepared by alkaline hydrolysis. In the ^{13}C NMR spectrum of **6** in $CDCl_3$, the carbon signal responsible for C-9 in the original compound was clearly observed and C–H long-range correlations by HMBC spectrum revealed the structure of **6**.

The bonds between C-1′ and C-2′, C-3′ and C-4′ were uncertain, because both H-2′ and H-3′ appeared as equivalent doublet signals. Nor did they exhibit C–H long-range correlation to C-4′. However, C–H long-range correlations between H-2′ and C-1′, H-2′ and the carbonyl carbon of the acetyl group (δ 170.3), H-3′ and C-1′ were

Table 3 ^{1}H and ^{13}C NMR signal assignments of F-16438 E (**3**) and F-16438 F (**4**) in pyridine-d_5

Position	F-16438 E (**3**)		F-16438 F (**4**)	
	δ_C	δ_H	δ_C	δ_H
1	174.6 (s)		174.6 (s)	
2	115.3 (s)		115.4 (s)	
3	163.9 (s)		163.9 (s)	
4	116.8 (d)	7.16 (1H, d, 8.3 Hz)	116.8 (d)	7.17 (1H, d, 8.0 Hz)
5	133.7 (d)	7.40 (1H, dd, 7.3, 8.3 Hz)	133.6 (d)	7.40 (1H, dd, 7.3, 8.0 Hz)
6	123.0 (d)	6.86 (1H, d, 7.3 Hz)	122.9 (d)	6.86 (1H, d, 7.3 Hz)
7	139.6 (s)		139.6 (s)	
8	48.6 (t)	4.22 (2H, s)	48.8 (t)	4.23 (2H, s)
9[a)]				
10	42.3 (t)	2.60 (2H, t, 7.5 Hz)	42.3 (t)	2.61 (2H, t, 7.5 Hz)
11	24.2 (t)	1.72 (2H, m)	24.2 (t)	1.72 (2H, m)
12～22	29.7～30.0 (t)	1.19～1.26 (22H[b)])	29.7～30.0 (t)	1.16～1.32 (22H[b)])
23	25.7 (t)	1.36 (1H, m), 1.51 (1H, m)	25.7 (t)	1.36 (1H, m), 1.49 (1H, m)
24	36.3 (t)	1.51 (1H, m), 1.72 (1H, m)	36.3 (t)	1.49 (1H, m), 1.72 (1H, m)
25	71.9 (d)	5.28 (1H, m)	72.0 (d)	5.28 (1H[b)])
26	20.2 (q)	1.36 (3H, d, 6.2 Hz)	20.2 (q)	1.36 (3H, d, 6.0 Hz)
1′	170.9 (s)		170.8 (s)	
2′	74.0 (d)	5.69 (1H, d, 9.5 Hz)	73.9 (d)	5.66 (1H, d, 9.5 Hz)
3′	70.4 (d)	5.23 (1H, d, 9.5 Hz)	70.1 (d)	5.11 (1H, d, 9.5 Hz)
4′	69.8 (d)	4.47 (1H, d, 9.2 Hz)	69.8 (d)	4.37 (1H, m)
5′	79.0 (d)	4.80 (1H, m)	76.0 (d)	4.93 (1H, m)
6′	63.2 (t)	4.63 (2H, m)	66.6 (t)	4.77 (1H, dd, 7.3, 11.3 Hz)
				5.28 (1H[b)])
2′-OAc	170.3 (s)		170.3 (s)	
	20.2 (q)	1.82 (3H, s)	20.2 (q)	1.79 (3H, s)
1″	99.6 (d)	5.58 (1H, s)	99.7 (d)	5.58 (1H, s)
2″	73.5 (d)	6.13 (1H, d, 3.3 Hz)	73.2 (d)	6.25 (1H, d, 1.8 Hz)
3″	73.6 (d)	4.25 (1H, dd, 3.3, 9.2 Hz)	73.6 (d)	4.39 (1H, m)
4″	69.6 (d)	4.38 (1H, m)	69.7 (d)	4.37 (1H, m)
5″	78.5 (d)	3.95 (1H, m)	78.4 (d)	4.01 (1H, m)
6″	63.2 (t)	4.29 (1H, dd, 7.7, 11.4 Hz)	63.3 (t)	4.26 (1H, dd, 7.7, 11.0 Hz)
		4.36 (1H, m)		4.60 (1H, dd, 1.9, 11.0 Hz)
2″-OAc	171.1 (s)		170.8 (s)	
	21.3 (q)	2.19 (3H, s)	21.2 (q)	2.14 (3H, s)
1‴			167.9 (s)	
2‴			42.8 (t)	3.78 (2H, s)
3‴			169.8 (s)	

[a)] ^{13}C signal was not clearly observed. [b)] Overlapped.

observed. The connectivity of these bonds was finally clarified by the analysis of the acetyl derivative of **3** (**7**). To distinguish between the original acetyl group signals in **3** and those introduced in the ^{1}H NMR spectrum, an acetic anhydride : acetic anhydride-d_6 (1 : 2) mixture was used for the acetylation. As a result, seven acetyl groups were incorporated into **3** and these methyl signals were observed to be about three times smaller than those of **3** in the ^{1}H NMR spectrum. The doublet signal of H-3′ changed to a doublet of doublets. That is to say, the coupling with H-4′ appeared in addition to the original coupling responsible for H-2′. These data clarified the bonds between C-1′ and C-2′, C-3′ and C-4′. Moreover, C–H long-range correlation between H-3′ and the carbonyl carbon of the chemically

Table 4 ^{1}H and ^{13}C NMR signal assignments of F-16438 G (**5**) in pyridine-d_5

Position	F-16438 G (**5**)	
	δ_C	δ_H
1	174.9 (s)	
2	117.1 (s)	
3	162.6 (s)	
4	115.5 (d)	7.14 (1H, d, 8.0 Hz)
5	132.8 (d)	7.39 (1H, dd, 7.5, 8.0 Hz)
6	121.8 (d)	6.91 (1H, d, 7.5 Hz)
7	146.4 (s)	
8	36.2 (t)	3.31 (2H, t, 7.5 Hz)
9	32.7 (t)	1.85 (2H, m)
10	30.3 (t)	1.48 (2H. m)
11～20	29.8～30.0 (t)	1.21～1.31 (20H[a])
21	25.7 (t)	1.36 (1H, m), 1.48 (1H, m)
22	36.3 (t)	1.48 (1H, m), 1.71 (1H, m)
23	72.0 (d)	5.28 (1H[a])
24	20.2 (q)	1.36 (3H, d, 6.0 Hz)
1′	170.8 (s)	
2′	73.9 (d)	5.66 (1H, d, 9.5 Hz)
3′	70.1 (d)	5.21 (1H, dd, 0.7, 9.5 Hz)
4′	69.8 (d)	4.37 (1H[a])
5′	76.0 (d)	4.93 (1H, m)
6′	66.6 (t)	4.77 (1H, dd, 7.0, 11.5 Hz)
		5.28 (1H[a])
2′-OAc	170.3 (s)	
	20.2 (q)	1.88 (3H, s)
1″	99.6 (d)	5.58 (1H, s)
2″	73.2 (d)	6.24 (1H, d, 2.2 Hz)
3″	73.6 (d)	4.39 (1H, m)
4″	69.7 (d)	4.37 (1H[a])
5″	78.5 (d)	4.01 (1H, m)
6″	63.3 (t)	4.27 (1H, dd, 7.7, 11.0 Hz)
		4.60 (1H, dd, 1.5, 11.0 Hz)
2″-OAc	170.8 (s)	
	21.2 (q)	2.15 (3H, s)
1‴	168.0 (s)	
2‴	42.8 (t)	3.78 (2H, s)
3‴	169.8 (s)	

[a] Overlapped.

introduced acetyl group was observed. Thus, the planar structure of **3** was elucidated as shown in Fig. 1.

The identifications of the sugar and aldonic acid were performed by GC-MS analysis of the silylated-cleavage product from treatment of **3** with 5% HCl - MeOH. By comparing the data with that of authentic standards, the sugar was determined to be mannose, and the aldonic acid

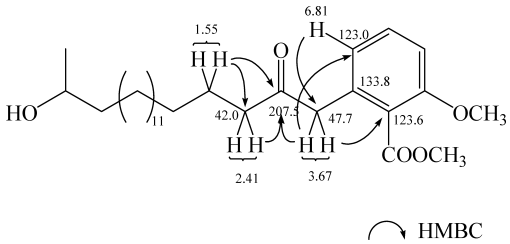

Fig. 2 Structure of the decomposition product of F-16438 E (**6**).

was found to be mannonic acid.

Structural Elucidations of Other Homologues

The structural elucidations of the homologues, **1**, **2**, **4** and **5** were carried out in the same way as F-16438 E (**3**).

The structural differences between **1** and **2** compared to **3** originated from the substituent pattern of the acetyl group at C-2′ or C-2″. By mass spectral analysis and NMR spectral analysis, the structures of **1** and **2** were elucidated as 2′,2″-dideacetylated and 2′-deacetylated derivatives of **3**, respectively (Fig. 1).

As shown in Fig. 1, the structure of **4** was determined to be the 6′-malonylated derivative of **3** by the characteristically isolated methylene signal in the ^{1}H NHR spectrum, its C–H long-range correlation to C-1‴ and C-3‴ and that of H-6′ to C-1‴.

In the case of **5**, it was characteristic that **5** possessed a two-methylene shorter alkyl chain without ketone at C-9 (Fig. 3).

The identification of the sugar and aldonic acid was also performed in the same way as **3**. As a result, the moieties in all four homologues of **3** were determined to be the same as **3**.

Discussion

In the course of our screening for binding inhibitors of CD44 and hyaluronic acid, F-16438 A (**1**), B (**2**), E (**3**), F (**4**) and G (**5**) were isolated from the cultured broth of *Gloeoporus dichrous* SANK 30502. The structures of compounds **1**～**4** were elucidated to be new compounds.

The structure of F-16438s resembles that of caloporoside [21] which has been reported to be an inhibitor of phospholipase C. The planar structure of **5** was determined to be a known 6′-malonylated derivative of caloporoside. The producing strain of caloporoside was reported as *Caloporus dichrous* (*Gloeoporus dichrous*) Strain 8365 and 8366. The strain producing **1**～**4** was also classified

to be *Gloeoporus dichrous* as a result of the taxonomic study. Interestingly, strain SANK 30502 did not produce caloporoside itself. Although we detected two other homologues named F-16438 C and D, their production titers were too low to investigate further chemical and biological studies about them.

NMR analysis of F-16438s was performed in pyridine-d_5, because other solvents did not give good resolution. However, pyridine still did not provide a clear signal at C-9. Analysis of the alkaline hydrolysis product (**6**) by mass spectrometry and several NMR techniques obtained in $CDCl_3$, elucidated it to be a ketone at the C-9 position. We predicted that keto-enol tautomerism occurred at C-9 in pyridine causing significant line broadening of the C-9 resonance; pyridine could influence the rate of interconversion of the two tautomers on the NMR time scale.

Since the stereochemistry of mannose, the mannonic acid moiety and the C-25 positions of **1**, **2**, **3**, **4** and **5** were not clear, further study is needed to clarify the similarities and differences of caloporoside with F-16438s. Because the optical rotations of **2**, **3**, **4** and **5** except for **1** were very similar to that of caloporoside, they may also have the same stereochemistry as caloporoside.

Experimental

General Experimental Procedures

IR spectra were obtained with a JASCO FT/IR-610 spectrometer. UV spectra were recorded on a Shimadzu UV-265FW spectrometer. NMR spectra were recorded on a Bruker Biospin AVC500 spectrometer equipped with a cryogenic probe. High resolution mass spectra were recorded on a Micromass LCT spectrometer. GC-MS spectra were recorded on a HP6890 Series GC System equipped with a column (Agilent Technologies, DB-5 0.25mm i.d.×15 m) and a 5973 Mass Selective Detector. LSI-MS spectra were recorded on a AutoSpec-Ultima (Waters).

Methyl 2-(18-Hydroxy-2-oxononadecyl)-6-methoxybenzoate (6)

To the methanol solution of **3** (15 mg/100 μl) was added 0.2 N KOH (1 ml) and the mixture was stirred at room temperature. The reaction was quenched by the addition of 1 N HCl to acidify at pH 3.0 and the resulting residue was extracted with ethyl acetate. The organic layer was washed with brine, dried over anhydr. Na_2SO_4, and concentrated to dryness to give an oily substance (5.4 mg). To the methanol solution of the oily substance was added diazomethane in ether. The residue was concentrated to dryness and purified by preparative HPLC using an ODS column (Waters, SYMMETRY C18 19 i.d.×100 mm). The chromatography was performed with 90% aq. MeCN in 5 mM $HCOONH_4$-HCOOH (pH 3.0) at a flow rate of 6 ml/minute to give **6** (2.0 mg). LSI-MS (*m*/*z*): 469 $(M+Li)^+$. ^{1}H NMR (500 MHz, $CDCl_3$, TMS): δ 1.19 (3H, d, J=6.0 Hz), 1.20～1.40 (overlapped), 1.42 (2H, m), 1.55 (2H, m), 2.41 (2H, t, J=7.5 Hz), 3.67 (2H, s), 3.84 (3H, s), 3.88 (3H, s), 6.81 (1H, d, J=7.5 Hz), 6.87 (1H, d, J=8.5 Hz), 7.33 (1H, t, J=7.5 Hz). ^{13}C NMR (125 MHz, $CDCl_3$, TMS): δ 23.5, 23.7, 25.8, 29.1～29.7 (overlapped), 39.4, 42.0, 47.7, 52.2, 56.0, 68.2, 110.1, 123.0, 123.6, 130.9, 133.8, 157.1, 168.2, 207.5.

Acetylation of 3

To the solution of **3** (5.6 mg) in pyridine (600 μl) was added an acetic anhydride : acetic anhydride-d_6 (1 : 2) mixture (300 μl, dropwise). The mixture was stirred at room temperature for 15 hours. The residue was concentrated to dryness and purified by preparative HPLC using an ODS column (Waters, SYMMETRY C18 19 i.d.×150 mm). The chromatography was performed with MeCN - 0.3% TEAP buffer at pH 3.0 (9 : 1) at a flow rate of 6 ml/minute. The acetyl derivative of **3** (**7**) was extracted with ethyl acetate and the organic layer was washed with brine, dried over anhydr. Na_2SO_4, and concentrated to dryness, yielding 4.9 mg of **7**. ^{1}H NMR (500 MHz, $CDCl_3$, TMS): δ 1.19 (3H, d, J=6.5 Hz), 1.20～1.38 (overlapped), 1.47 (1H, m), 1.60 (1H, m), 1.66 (2H, m), 2.00*, 2.05*, 2.07*, 2.08*, 2.08*, 2.10*, 2.12 (3H, s), 2.23 (3H, s), 2.42*, 2.48 (2H, t, J=7.5 Hz), 3.64 (1H, m), 3.95 (1H, dd, J=4.5, 13.0 Hz), 4.12 (1H, m), 4.15 (1H, m), 4.21 (1H, m), 4.40 (1H, dd, J=2.0, 12.5 Hz), 4.86 (1H, s), 4.93 (1H, m), 5.02 (1H, d, J=8.0 Hz), 5.04 (1H, dd, J=3.0, 10.0 Hz), 5.19 (1H, t, J=10.0 Hz), 5.41 (1H, d, J=2.5 Hz), 5.45 (1H, dd, J=2.6, 8.3 Hz), 5.49 (1H, dd, J=2.6, 7.7 Hz), 6.24 (1H, s), 7.07 (1H, d, J=8.0 Hz), 7.23 (1H, d, J=8.0 Hz), 7.65 (1H, t, J=8.0, 8.0 Hz). ^{13}C NMR (125 MHz, $CDCl_3$, TMS): δ 19.3, 20.5～20.8 (overlapped), 25.2, 26.8, 29.0, 29.3, 29.5～29.7 (overlapped), 33.4, 35.7, 60.7, 62.7, 66.1, 68.2, 68.6, 68.7, 69.5, 70.9, 71.9, 72.7, 73.3, 95.5, 102.7, 112.9, 121.8, 123.1, 135.4, 140.1, 151.9, 159.1, 159.6, 166.9, 168.9*, 169.2*, 169.6, 169.6*, 169.8*, 170.0*, 170.6*, 170.7, 170.7*. * Chemically introduced acetyl groups.

Identification of Mannose and Mannonic Acid

The 5% HCl - MeOH solution (500 μl) was added to 1 mg of **1**, **2**, **3**, **4**, **5** and authentic samples (mannose and mannonic acid γ-lactone), respectively. Each mixture was sealed to the ampul and heated at 75°C for 5 hours. After

that, these samples were cooled to room temperature and dried *in vacuo*. Then each decomposition product was dissolved in pyridine (1 ml). To the solution (50 μl) was added *N*,*O*-bis(trimethylsilyl)trifluoroacetamide (BS-TFA, 80 μl) and it was then analyzed by GC-MS.

Acknowledgments We are deeply grateful to Dr. Toshio Takatsu for useful advice.

References

1. Abatangelo G, O'Regan M. Hyaluronan: biological role and function in articular joints. Eur J Rheumatol Inflamm 15: 9–16 (1995)
2. Brandt KD, Smith GN Jr, Simon LS. Intraarticular injection of hyaluronan as treatment for knee osteoarthritis. What is the evidence? Arthritis Rheum 43: 1192–1203 (2000)
3. Dahl LB, Dahl IMS, Engström-Laurent A, Granath K. Concentration and molecular weight of sodium hyaluronate in synovial fluid from patients with rheumatoid arthritis and other arthropathies. Ann Rheum Dis 44: 817–822 (1985)
4. Ghosh P. The role of hyaluronic acid (hyaluronan) in health and disease: interactions with cells, cartilage and components of the synovial fluid. Clin Exp Rheumatol 12: 75–82 (1994)
5. De la Motte CA, Hascall VC, Drazba J, Bandyopadhyay SK, Strong SA. Mononuclear leukocytes bind to specific hyaluronan structures on colon mucosal smooth muscle cells treated with polyinosinic acid: polycytidylic acid: inter-alpha-trypsin inhibitor is crucial to structure and function. Am J Pathol 163: 121–133 (2003)
6. Majors AK, Austin RC, de la Motte CA, Pyeritz RE, Hascall VC, Kessler SP, Sen G, Strong SA. Endoplasmic reticulum stress induces hyaluronan deposition and leukocyte adhesion. J Biol Chem 278: 47223–47231 (2003)
7. Toole BP. Hyaluronan promotes the malignant phenotype. Glycobiology 12: 37–42 (2002)
8. Toole BP, Hascall VC. Hyaluronan and tumor growth. Am J Pathol 161: 745–747 (2002)
9. Udabage L, Brownlee GR, Nilsson SK, Brown TJ. The over-expression of HAS2, Hyal-2 and CD44 is implicated in the invasiveness of breast cancer. Exp Cell Res 310: 205–217 (2005)
10. Lesley J, Hyman R, Kincade PW. CD44 and its interaction with extracellular matrix. Adv Immunol 54: 271–335 (1993)
11. Picker LJ, Nakache M, Butcher EC. Monoclonal antibodies to human lymphocyte homing receptors define a novel class of adhesion molecules on diverse cell types. J Cell Biol 109: 927–937 (1989)
12. Bourguignon LYW, Lokeshwar VB, He J, Chen X, Bourguignon GJ. A CD44-like endothelial cell transmembrane glycoprotein (GP116) interacts with extracellular matrix and ankyrin. Mol Cell Biol 12: 4464–4471 (1992)
13. Zhu D, Bourguignon LYW. Overexpression of CD44 in pl85(neu)-transfected NIH3T3 cells promotes an up-regulation of hyaluronic acid-mediated membrane-cytoskeleton interaction and cell adhesion. Oncogene 12: 2309–2314 (1996)
14. Brown TA, Bouchard T, St John T, Wayner E, Carter WG. Human keratinocytes express a new CD44 core protein (CD44E) as a heparan-sulfate intrinsic membrane proteoglycan with additional exons. J Cell Biol 113: 207–221 (1991)
15. Grover J, Roughley PJ. Expression of cell-surface proteoglycan mRNA by human articular chondrocytes. Biochem J 309: 963–968 (1995)
16. Culty M, Nguyen HA, Underhill CB. The hyaluronan receptor (CD44) participates in the uptake and degradation of hyaluronan. J Cell Biol 116: 1055–1062 (1992)
17. Hua Q, Knudson CB, Knudson W. Internalization of hyaluronan by chondrocytes occurs *via* receptor-mediated endocytosis. J Cell Sci 106: 365–375 (1993)
18. Tammi R, Rilla K, Pienimaki JP, MacCallum DK, Hogg M, Luukkonen M, Hascall VC, Tammi M. Hyaluronan enters keratinocytes by a novel endocytic route for catabolism. J Biol Chem 276: 35111–35122 (2001)
19. Harada H, Nakata T, Hirota-Takahata Y, Tanaka I, Nakajima M, Takahashi M. F-16438s Novel Binding Inhibitors of CD44 and hyaluronic acid I. Establishment of an assay method and biological activity. J Antibiot 59: 753–769
20. Núñez M, Ryvarden L. East Asian polypores. Synopsis Fungorum 14: 315–317 (2001).
21. Weber W, Schu P, Anke T, Velten R, Steglich W. Caloporoside, a new inhibitor of phospholipases C from *Caloporus dichrous* (Fr.) Ryv. J Antibiot 47: 1188–1194 (1994)